Cell

Meiotic Chromosomes Move by Linkage to Dynamic Actin Cables with Transduction of Force through the Nuclear Envelope

R. Koszul,[1] K.P. Kim,[1] M. Prentiss,[2] N. Kleckner,[1,*] and S. Kameoka[1]
[1]Department of Molecular and Cellular Biology
[2]Department of Physics
Harvard University, Cambridge, MA 02138, USA
*Correspondence: kleckner@fas.harvard.edu
DOI 10.1016/j.cell.2008.04.050

SUMMARY

Chromosome movement is prominent during meiosis. Here, using a combination of in vitro and in vivo approaches, we elucidate the basis for dynamic mid-prophase telomere-led chromosome motion in budding yeast. Diverse findings reveal a process in which, at the pachytene stage, individual telomere/nuclear envelope (NE) ensembles attach passively to, and then move in concert with, nucleus-hugging actin cables that are continuous with the global cytoskeletal actin network. Other chromosomes move in concert with lead chromosome(s). The same process, in modulated form, explains the zygotene "bouquet" configuration in which, immediately preceding pachytene, chromosome ends colocalize dynamically in a restricted region of the NE. Mechanical properties of the system and biological roles of mid-prophase movement for meiosis, including recombination, are discussed.

INTRODUCTION

Movement plays fundamental roles in basic chromosomal processes. Organized chromosomes congress and segregate at mitosis. Movement also occurs during DNA replication, DNA repair, gene activation, and transcription and also globally (reviewed in Kumaran et al., 2008). Movement is especially significant during meiosis, when homologous maternal and paternal chromosomes ("homologs") must recognize one another and "pair," efficiently and without entanglements.

Meiotic homolog juxtaposition culminates in formation of the synaptonemal complex (SC) between homolog axes all along their lengths. SC formation defines "zygotene"; presence of complete SC defines "pachytene." Pachytene chromosomes are well-organized, with chromatin loops of homologs emanating outward from either side of the SC. Zygotene and pachytene also include global changes in chromosome disposition. Before zygotene, chromosome ends associate with the NE in meiosis-specific complexes. During zygotene, these ends cluster into a localized area of the NE (the "bouquet") while, at early pachytene, they redistribute throughout the nuclear periphery (Zickler and Kleckner, 1998; Bass, 2003; Scherthan 2007; Harper et al., 2004). Zygotene and pachytene chromosomes also exhibit dynamic movements over shorter time scales. Such movements have been described thus far in rat spermatocytes (Parvinen and Soderstrom, 1976), *S. pombe* meiosis (reviewed in Chikashige et al., 2007) and budding yeast (Trelles-Sticken et al., 2005; Scherthan et al., 2007; this work; Conrad et al., 2008; A. Shinohara, personal communication), and *C. elegans* (A. Dernburg, personal communication).

In pombe, telomeres cluster at the spindle pole body (SPB) and are moved dramatically back and forth along microtubules via dynein motors (Yamamoto et al., 1999; Chikashige et al., 2007); in budding yeast, both telomeres and actin are implicated (references above). The current study further examines meiotic chromosome movement in budding yeast with respect to mechanism and biological significance.

RESULTS

Active Chromosome Movement Is Required In Vivo to Overcome Constraints on Thermal Motion

Mechanical Properties of In Vitro Pachytene Chromosomes

We developed a method to release pachytene chromosomes as singlets and interconnected groups (Figure 1A; Movies S1 and S2 available online). Compared to in vivo counterparts, in vitro DAPI-stained chromosomes present a similar length (1.3 μm versus 1.1 μm; n = 30) and are slightly wider (0.4–0.6 μm versus ~0.35–0.4 μm), perhaps reflecting slight chromatin decondensation. Singlet chromosomes exhibit a random walk path with step-sizes conforming to a Gaussian distribution (Figure 1Bi). In vitro chromosomes also exhibit thermal bending, which, for any filament, reflects its intrinsic stiffness/flexibility as discussed in terms of "persistence length" (Lp). Lp is the distance over which the correlation between the directions of two vectors tangent to the skeleton path of the polymer is lost (Doi and Edwards, 1986). Appropriate analysis of singlet in vitro pachytene chromosomes (n = 40) (Ott et al., 1993; Figure 1Bii; Supplemental Data, Note S1) defines a set of (Gaussian-distributed) bending angles (Figure 1Biii,

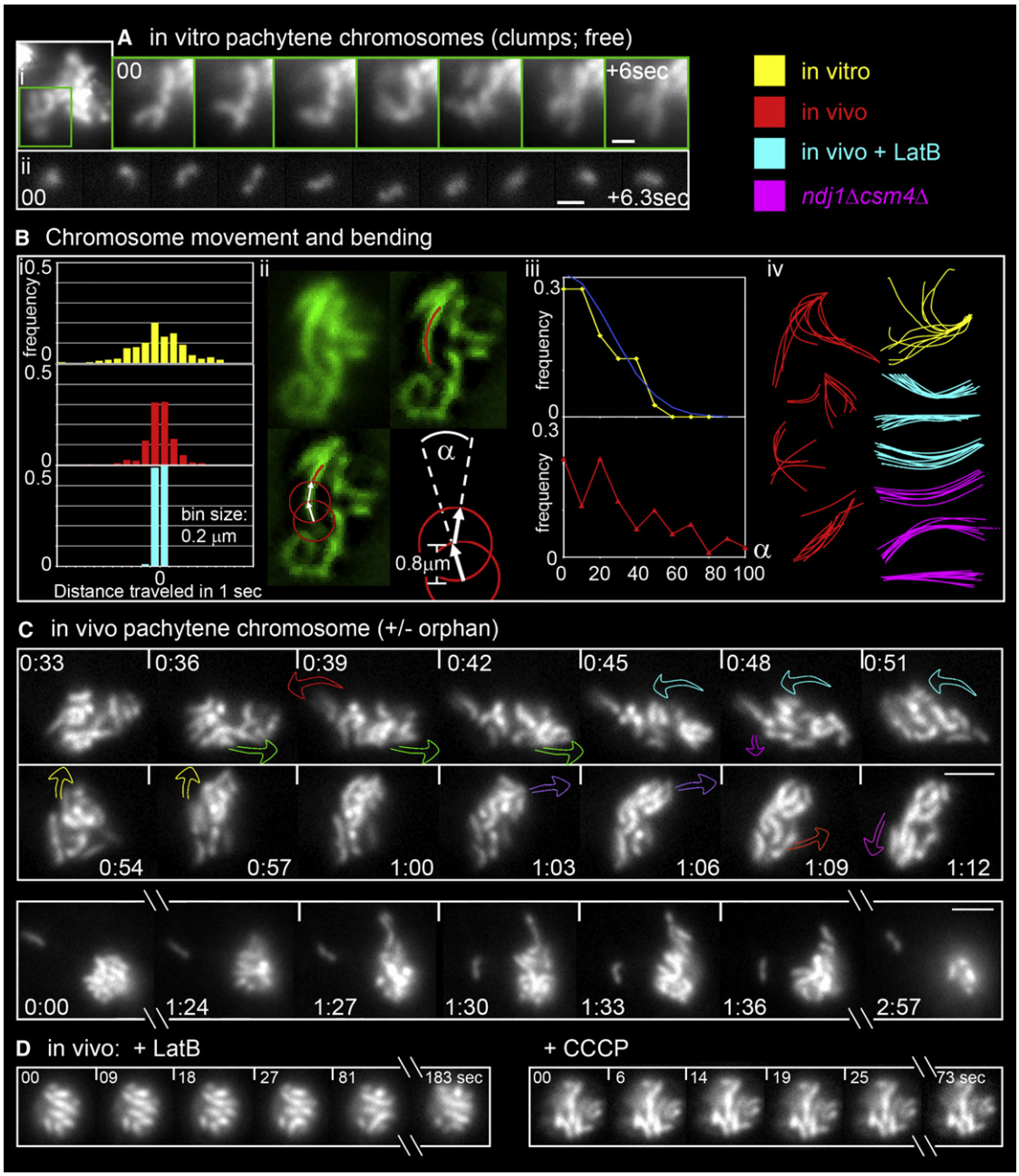

Figure 1. In Vivo and In Vitro Properties of Pachytene Chromosomes

(A) Time series, nondeconvolved, of DAPI-labeled in vitro chromosomes. (i) individual chromosomes emerging from the compact mass of a partially disrupted nucleus (1 s intervals; Movie S1). (ii) free chromosome released from disrupted nucleus (0.7 s intervals; Movie S2).

(B) (i) Step-size histograms of the displacement of in vitro (yellow), in vivo (red), and in vivo + LatB (turquoise) pachytene chromosome ends, tracked every second for 91, 60, and 60 s, respectively. (ii) Calculation of bending angles and persistence lengths. Images of Zip1-GFP-labeled chromosomes (top left) were deconvolved and the skeleton paths of lengthy chromosome segments were outlined manually (top right, red line). Consecutive tangent vectors were then drawn beginning at one end of the chromosome using an arc length of 0.8 μm (bottom left; Note S1). The angle α between two vectors is then determined (bottom right). For in vitro chromosomes, these angles are used to calculate persistence length (Lp). (iii) Distributions of (α) (in absolute values within 0°–180°) for in vitro (yellow; n = 40 chromosomes; corresponding normal curve in blue) and in vivo chromosomes (red; n = 50). (iv) Representative series of chromosome outlines taken every second over 8–10 s and superimposed.

(C) Two-dimensional time series of pachytene Zip1-GFP chromosomes (5–6 hr after meiosis induction; 3 s intervals; strain NKY3834). Top: Movie S3; colored arrows indicate abrupt, discrete transition(s) (see Figures 2Ai and 2Aii). Bottom: Movie S4 illustrates long-lived orphan plus dramatic outward protrusion (1:27–1:36).

(D) Same as (A) but with 30 μM LatB (left) or 40 μM CCCP (right). (A) Scale bar = 1 μm. (C and D) Bars = 2 μm.

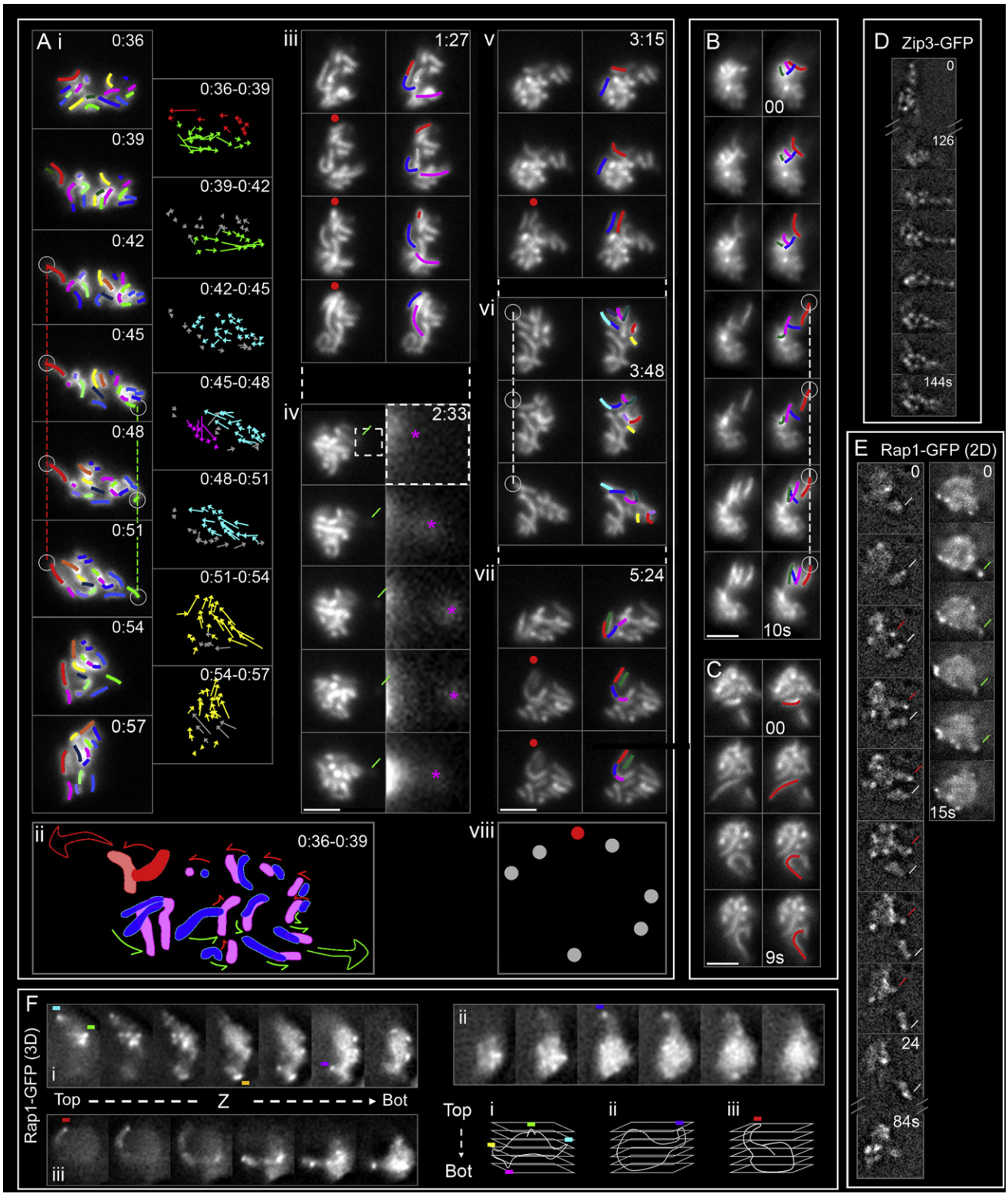

Figure 2. Pachytene Chromosome Motion

Two-dimensional time series of Zip1-GFP chromosomes (bars = 2 μm) and analysis. (Ai and Aiii–Avii: same nucleus as Figure 1C [top]; Movie S3; 3 s intervals. B and C: Movies S9 and S10; 1 s intervals).

yellow curve) that in turn define Lp = ~12 μm (Note S1), a value characteristic of a "semiflexible" object (Discussion).

Actively Promoted Dynamic Movements In Vivo

Scherthan et al. (2007) showed that pachytene Zip1-GFP chromosomes in living cells exhibit dynamic, dramatic motion over time intervals of a few seconds. We confirmed this observation (e.g., Figure 1C top, Movie S3) and noticed that sometimes a single chromosome becomes well separated from the main group (5 occurrences in 100 nuclei over 3 min). "Orphans" usually persist ≤5 s but occasionally "dangle in space" much longer (Figure 1C bottom, Movie S4).

Chromosome movements in vivo are similar to those in vitro, suggesting that in vivo movements might be thermally promoted. This is not the case: Scherthan et al. (2007) find that in vivo motion is inhibited by LatrunculinB (LatB), which binds to actin monomers and prevents their incorporation into filaments. We also see this effect (Figure 1D; e.g., Movie S5, n > 100) and, further, have found that inhibition is a specific effect of LatB on actin: a mutant whose actin no longer binds LatB is resistant to its effects (Figure S1). LatB severely reduces both translational step-sizes (Figure 1B, compare red and turquoise) and bending angles (Figure 1Biv, turquoise versus red; data not shown). We also find that movement is inhibited by carbonyl cyanide m-chloro phenyl hydrazone (CCCP), which blocks mitochondrial ATP synthesis (Figure 1D; e.g., Movie S6, n > 100; Experimental Procedures). In contrast, neither inhibition of microtubule (MT) polymerization by nocodazole nor deletion of the cytoplasmic dynein-encoding gene *DHC1* detectably reduces pachytene motion (Movie S7; data not shown), implying a fundamentally different mechanism from that described for pombe (Introduction).

In Vivo Constraints

Chromosome movement in vivo in the presence of LatB/CCCP is also much less dynamic than movement in vitro (Figure 1A versus 1D; Figures 1Bi and 1Biv, turquoise versus yellow). This difference suggests that, in vivo, spontaneous thermal motions are severely constrained such that an active mechanism is required to provide significant displacement. Interestingly, in vivo chromosomes often exhibit bending angles greater than any observed during spontaneous movement (Figure 1Biii, red versus yellow); thus, actin-mediated forces must be significantly greater forces than thermal forces. Also, abrogation of telomere/NE tethering (by the *ndj1Δ* mutation; below) does not restore vigorous movement to chromosomes in motion-defective conditions (e.g., *ndj1Δ csm4Δ*, Figure 1Biv pink; or *ndj1Δ* + LatB, data not shown), implying that constraints on spontaneous movement reflect conditions internal within the nucleus.

Dissection of In Vivo Chromosome Motion

Analysis of individual Zip1-GFP chromosome paths over time reveals five features of pachytene movement.

(1) Abrupt, Discrete, Directed Transitions of Chromosome Groups

A given nucleus experiences a series of abrupt, discrete transitions. In each, a group of nearby chromosomes (or sometimes a single chromosome) moves coordinately in an outward-directed and/or peripheral and curvilinear path. Eight transitions are indicated in Figure 1C (top; Movie S3); five of these are documented by color-coding of individual chromosomes and sets of colored arrows describing frame-to-frame displacements (Figures 2Ai and 2Aii). Movie S3 and other movies (below; Figure S2) show that a given nucleus exhibits one transition every ~6–9 s, with each transition lasting <3–9 s. A nucleus sometimes experiences two transitions simultaneously. However, such pairs are only partially contemporaneous, involve different sets of chromosomes, and occur in different directions, implying that they are independent events (e.g., red versus green arrows and magenta versus pink arrows in Figures 1C, 2Ai, and 2Aii). The dramatic nature of transitions is further illustrated by Figure 1D (1:24–1:36) (Movie S4); illumination of recombination-related Zip3-GFP foci (Figure 2D; Movie S8) (Agarwal and Roeder, 2000); and examples below.

(2) Telomere-Led Movement of a "Lead" Chromosome

In many transitions, a chromosome located at the leading edge of motion moves dramatically, and in a way that strongly suggests that force is being exerted specifically on its "leading end." Such effects are indicated by red chromosomes in Figure 2 (Figures 2Ai [0:36–0:39], 2Aiii, and 2Av–2Avii; cartoon 2Aii); Figure 2B top four panels (Movie S9); Figure 2C, plus additional dramatic examples in the same series (Movie S10). A leading end typically moves 0.5 to 1 μm (and up to 2 μm) at ~0.3–0.5 μm per second (up to ~0.8 μm/s). No particular chromosome(s) occur preferentially as "leaders," as all possible sizes of chromosomes are seen in this role. "Maverick" chromosomes noted by Scherthan et al. (2007) correspond to leaders exhibiting especially accentuated displacement.

(A) (i) Left column: all chromosomes in the focal plane are outlined (left column; red color stands for "leaders"). Vertical dashed lines indicate anchoring of leader (red) and putative leader (green) chromosomes. Right column: for each chromosome, the direction and range of motion are depicted by vectors drawn between apparent telomeric positions in successive frames with different colors denoting different transitions. (ii) Stylized depiction of motion seen in (i) (0:36-0:39) with positions in blue and pink, respectively (leader in red) and directional effects implied by arrows. (Aiii–Avii) and (B and C): Seven additional discrete transitions. Chromosomes undergoing dramatic movement are highlighted, with red color representing the leader (see also Movie S10). Green line indicates an orphan (magnification at right, pink asterisk). Red dots highlight repeated use of a single trajectory in independent transitions. Open circle and dotted line indicate "anchoring." (Aviii) Summary of all focal points over 6 min for Movie S3 (see also Figure S2).

(D) Time series for a Zip3-GFP nucleus (NKY3501).

(E) Two-dimensional dynamics of Rap1-GFP signals in nuclei of two living cells (NKY4000). Telomeres positions marked by stronger GFP foci; chromatin shape given by general background. Three second intervals except at discontinuous points (Movie S11). Left and middle: deconvolved frames showing a long transient nuclear protrusion with a GFP telomere focus at its extremity (red line), and an orphan chromosome (white line). Right: nondeconvolved frames of a short chromatin protrusion with a telomere at the edge (green line).

(F) Three-dimensional reconstructions of chromatin protrusions revealed by Rap1-GFP. Top: consecutive 0.4 μm optical "Z" sections taken at 600 ms intervals, from top to bottom, of three nuclei (i–iii). Chromatin protrusions (and essentially all protrusions in such analyses) have telomeric GFP foci at their outer extremities (colored squares). Bottom: schematic 3D reconstruction of each nucleus.

(3) Coordinated Movement via Interconnections among the Lead Chromosome and Others

In transitions involving multiple chromosomes, the followers (nonred chromosomes in all transitions shown in Figures 2Ai, 2Aiii, 2Av–2Avii, 2B, and 2C) reorient and move in the direction defined by the leader (arrows in Figures 2Ai and 2Aii; nonred chromosomes in other panels). When two transitions occur simultaneously, chromosomes located between the two moving groups respond to both tendencies (middle chromosomes, Figure 2Aii). Some transitions involve movement only of a lead chromosome, occasionally yielding a well-isolated "orphan" (e.g., Figure 2Aiv).

Coordinately moving chromosomes always comprise a spatially associated group (e.g., Figures 2A–2C). Often, chromosomes nearer to the lead chromosome exhibit greater movement than those located farther away (e.g., relative magnitudes of arrows in Figure 2Ai; relative movements of nonred chromosomes in other transitions of Figures 2A–2C). Nonetheless, spatial proximity to the lead chromosome is not sufficient to determine coordinate movement: motion often involves one group of chromosomes close to the lead chromosome without involving others equally close (Figure 2Avi). Also, affected chromosomes sometimes form a chain that follows the lead chromosome like a string of sausages (Figures 2Aiii and 2Avii). Such phenomena suggest that movement of the lead chromosome provokes movement of a subset of nearby chromosomes that happen to be interconnected.

(4) Peripheral Tracks

Other phenomena point to involvement of stably positioned extranuclear "tracks." (1) A chromosome can move back and forth along a particular trajectory (Figure 2Aiv). (2) Directed movement of one chromosome can be followed, shortly afterward, by directed movement of another chromosome(s) along the same trajectory (Figure 2B, first four frames versus last three frames). (3) Independent discrete transitions, separated by many seconds or minutes, occur along the same or closely adjacent trajectories (Figures 2Aiii, 2Av, and 2Avii). The focal points defined for a single nucleus over several minutes seem to define short linear arrays (Figures 2Aviii and S2), implying different focal points along a single "track" and/or drifting of a single focal point.

(5) Lead Chromosome Movement Often Culminates in Spatial Fixation

Leader chromosome ends also tend, at the end of the transition, to become fixed in space (dotted vertical lines, Figures 2Ai, 2Avi, and 2B). An end that has become fixed sometimes remains so until a major transition occurs in a different direction, whereupon it moves away in the new direction (Figure 2Ai, red and green vertical lines until "yellow" transition at 0:51–0:54). It appears that spatially fixed chromosome ends are physically anchored to an external structure from which they are eventually released when pulled away by the force of another transition. Such associations could also explain dangling of orphans at fixed positions (Figure 1D).

Telomeres Occur at the Leading Ends of Chromosomal Protrusions

We also examined dynamic behavior of Rap1-GFP, which localizes prominently to chromosome telomeres and less prominently throughout the chromosomes (Klein et al., 1992; Trelles-Sticken et al., 2005), thus permitting differential visualization of both features. Two-dimensional (2D) movies reveal dynamic, outward-directed chromatin protrusions, essentially every one of which has a bright (telomeric) focus at its leading point (Figure 2E; Movie S11). Correspondingly, three-dimensional (3D) reconstructions of entire nuclei, via images obtained from living cells by rapid collection of optical z-sections (streaming), reveal long protrusions with bright foci at their leading ends (Figure 2F). These results confirm that chromosome movement is telomere led.

The NE Undergoes Local Shape Changes in Correlation with Chromosome Movement

Since pachytene chromosome ends are robustly associated with the NE (Introduction), telomere-led chromosome movement should be accompanied by concomitant local NE deformation. Two-dimensional timelapse analysis of nuclear pores illuminated with Nup49-GFP (Belgareh and Doye, 1997) show this to be true.

Cones that Give Rise to Short and Long Protrusions

In vegetative growth or early meiosis, the NE exhibits a static spherical or oval shape (Heun et al., 2001). In contrast, the pachytene NE exhibits highly dynamic local shape changes. Most common are outward-directed angular deformations (Figure 3Ai), which correspond to "cones" in 3D space. Many of these deformations then evolve into thin protrusions or "NE tubes," which fall into two length categories, "short" (up to ~0.3 μm; Figure 3Ai; Movie S12) and "long" (>> 0.3 μm; Figures 3Aii–3Aiv; Movies S13–S15). The two types are similar in diameter (~0.3–0.4 μm, n = 20 and n = 35, respectively), extend outward at similar velocities (~0.3–0.5 μm/s, n = 30 each), and are usually transient, though long tubes can be quite stable (>100 s).

Correlations with Chromosome Movement

Dynamic NE shape changes can be correlated with directional, telomere-led chromosome movement by direct covisualization with DAPI-stained chromosomes. As illustrated in the sequence of Figure 3B (see also Movie S16): (1) At 03–06 s, an angular deformation, likely with a short protrusion, occurs at the leading end of a single chromosome that protrudes from the main chromosome mass (pink lines). (2) At a different position in the nucleus, a DAPI signal (yellow arrow) undergoes outward-directed movement, accompanied by elongation of the surrounding NE segment (outlined with a red line inside the box). (3) This change is followed by movement of the body of the nucleus in the opposite direction via global "drift" (below), leaving behind an "anchored" DAPI signal plus an associated NE segment and an elongated NE connector (Figure 3B; 09–18 s). (4) The orphan eventually separates from the NE anchor point and moves to the main chromosome mass while the NE tube collapses (Figure 3B; 18–24 s).

NE shape changes and chromosome movements are correlated in other ways. Both are eliminated by CCCP or LatB, which cause the NE to assume a regular spherical shape (Figure 3D; Movies S17 and S18; below). Chromatin protrusions seen by Rap1-GFP or Zip3-GFP and NE tubes (short and long) have the same width (~0.4 ± 0.1 μm, n = 6 protrusions and n = 35 tubes) and emanate outward at the same velocity (0.3–0.5 μm/s; above). Finally, both effects initiate at the onset of zygotene and continue through the end of pachytene (below).

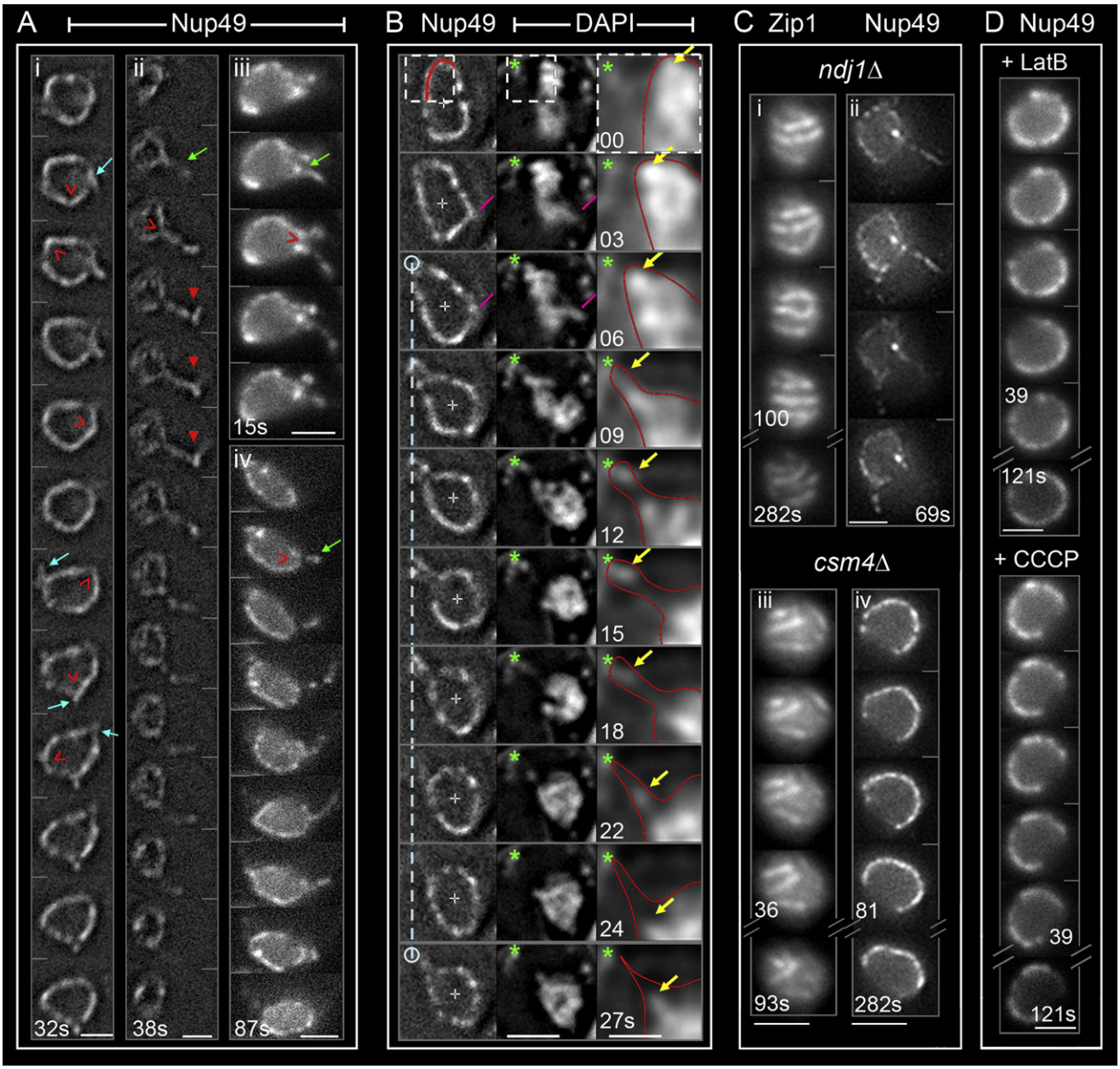

Figure 3. Pachytene Nuclear Envelope Dynamics

Two-dimensional time series of pachytene nuclei with Nup49-GFP-labeled NE, taken at two (Ai and Aii) or three (Aiii, Aiv, B, and C) second intervals. Scale bars = 2 μm.

(A) Deconvolved frames showing NE angular deformations (red empty arrowheads) eventually evolving into small (i) or long (ii–iv) transient protrusions (turquoise and green arrows indicate the birth of such protrusions, respectively). Long protrusions occasionally exhibit angular path (≥1%, n = 200; red arrowhead).

(B) Covisualization of chromosomes and NE (DAPI and Nup49-GFP, respectively; strain NKY3992). Pink lines indicate concomitant NE angular deformation and an outward-directed chromosome (deconvolved images). White dotted vertical line indicates "anchoring" of a NE region. The section corresponding to white dotted squares is magnified in the right column as a less contrasted, deconvolved image (red lines indicate NE outline). Yellow arrows indicate outward movement of a chromosome mass and emergence and movement of an orphan. Green asterisk indicates the continuous presence of a DAPI-stained mitochondrion.

(C) Dynamics of Zip1-GFP chromosomes and Nup49-GFP NE in *ndj1*Δ and *csm4*Δ pachytene cells (NKY3837, 3993, 4002, and 3994). Due to delayed progression of these mutants through meiosis, cells were examined at t = 6 hr and 7 hr after meiosis induction, respectively.

(D) Reduction of NE movements after addition of either 30 μM LatB (top) or 40 μM CCCP (bottom).

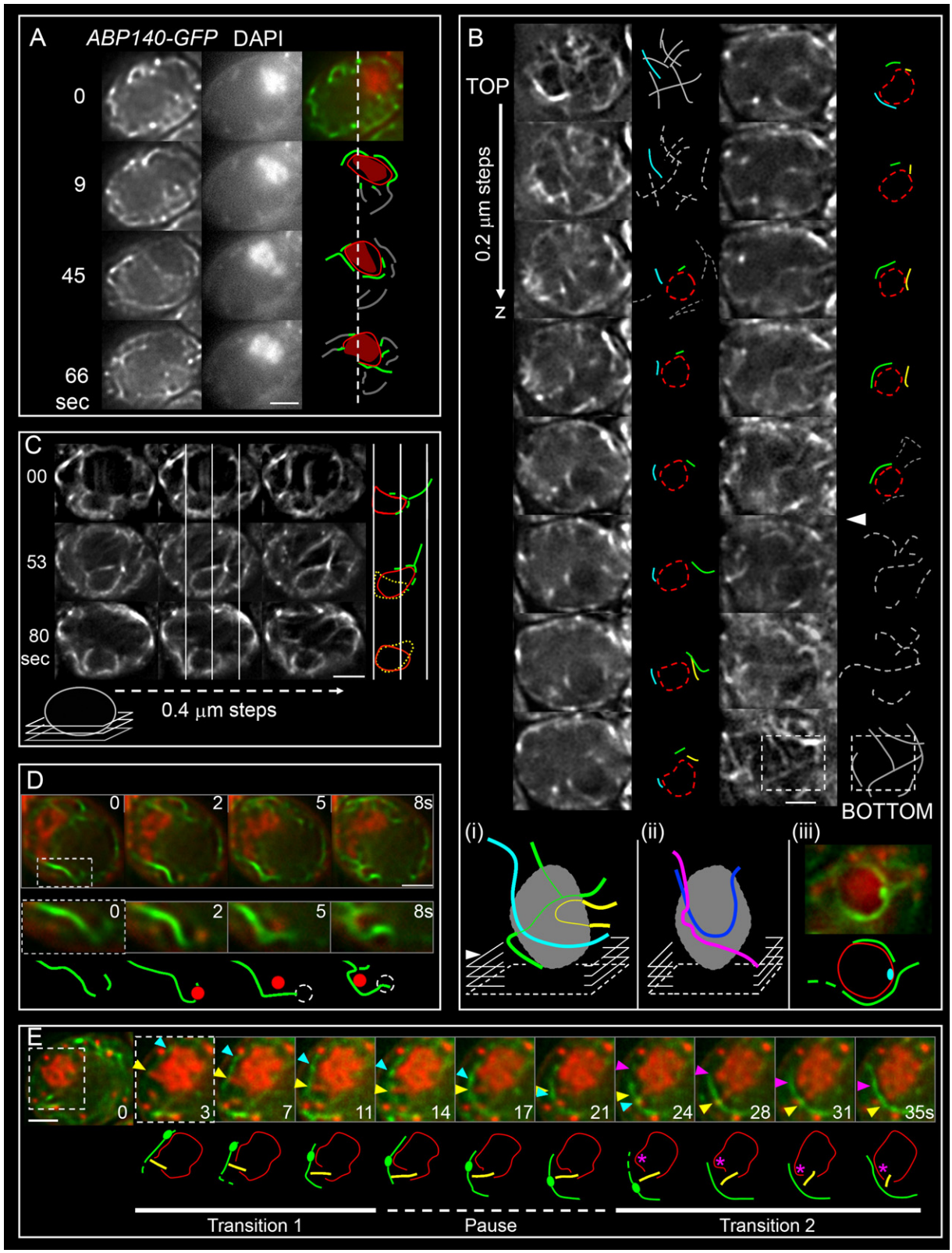
A
ABP140-GFP DAPI
0
9
45
66
sec
B
TOP
0.2 μm steps
z
BOTTOM
(i)
(ii)
(iii)
C
00
53
80
sec
0.4 μm steps
D
0
2
5
8s
E
0
3
7
11
14
17
21
24
28
31
35s
Transition 1
Pause
Transition 2

We conclude that directional force is exerted specifically on telomere/NE ensembles, moving the targeted chromosome end and concomitantly deforming the NE at the affected point.

Telomere/NE Uncoupling in ndj1Δ

Ndj1 localizes to chromosome ends and mediates their robust meiosis-specific association with the NE, though weaker mitotic-like associations are seen in its absence (Conrad et al., 1997; Trelles-Sticken et al., 2000). Pachytene chromosome motion is strongly reduced in *ndj1Δ* (Scherthan et al., 2007; Figure 3Ci; Movie S19; n = 150 nuclei during 3 min). Thus, robust telomere/NE association is required for active chromosome movement. In contrast, dynamic NE deformations still occur in *ndj1Δ,* similarly to WT (~40% of 100 nuclei over 3 min; Figure 3Ci; Movies S20 and S21), and are still LatB sensitive (data not shown). Thus, actin-mediated forces are exerted on the NE component of telomere/NE complexes, independent of meiosis-specific telomere association. Correspondingly, *ndj1Δ* chromosomes still exhibit significant residual movement (Movie S19), which is also eliminated by LatB (not shown), presumably via nonspecific chromosome/NE associations.

Aberrant Dynamics in *csm4Δ*

Csm4 is a putative tail-anchored membrane protein that interacts physically and functionally with Ndj1, localizes to the NE in mitotic and meiotic cells, and is strongly induced in meiosis (Conrad et al., 2008; B. Weiner, personal communication; A. Shinohara, personal communication). Csm4 is not required for robust telomere/NE association (R.K., unpublished data). Nonetheless, absence of Csm4 dramatically reduces not only pachytene chromosome motion, more than absence of Ndj1 (Figure 3Ciii; Movie S22), but also NE deformations, which are now sporadic and less pronounced than in either WT or *ndj1Δ* (Figure 3Civ; Movie S23). These phenotypes suggest that Csm4 couples telomere/NE ensembles to the force-generation process.

Identification of Actin Filaments that Hug the NE and Extend outward into the Global Cytoskeletal Network

We visualized actin cables illuminated by Abp140-GFP (Yang and Pon, 2002) in combination with DAPI-stained chromosomes, the NE (Nup49-GFP), and/or the SPB (via SPC42-YFP). Meiotic nuclei, unlike their mitotic counterparts, exhibit a complex, highly dynamic, nonpolarized cage-like network of cytoplasmic actin cables (Taxis et al., 2006). Two- and three-dimensional movies of living cells at times when most cells are in zygotene or pachytene (t = 4 or 5 hr after initiation of meiosis) confirm the existence of actin networks at both stages and reveal additional features common to both time points:

- The nucleus is a "black hole" within which no actin cables are visible (Figures 4A, 4B, and 4C; Movies S24 and S25). Also, irrespective of the highly dynamic nature of the cytoskeletal actin network and ongoing nucleus/chromosome shape changes, the nucleus is usually quite fixed within the cell, with occasional slow drift and abrupt movement (Figure S1).

- In every cell, a few cables make circumvolutions such that internal segments "hug" the external nuclear periphery, with their ends extending outward beyond the nucleus into the general cytoskeletal network. This pattern appears clearly in 3D reconstructions (Figure 4Bi; Movie S25) and correlates to 2D patterns (Figures 4A and 4C). Actin cable/NE association is very intimate: covisualization of Nup49-GFP and Abp140-GFP presents only a single nucleus-peripheral signal, even throughout dynamic nucleus shape changes (Figure 4C).

- Nucleus-hugging actin cables are located preferentially at/around point at which the nucleus is juxtaposed to the edge of the cell (Figure 4Bii). The SPB is also nearly always located at the nucleus/cell periphery interface (~84% of cells at t = 4 hr, n = 32; Figure 4Biii). It jiggles at a relatively stationary position over the time intervals monitored (1 min), with abrupt shifts occasionally observed (data not shown). These features may be due to cytoplasmic astral microtubules holding the SPB in a fixed position, similarly to nuclear positioning during mitosis (Shaw et al., 1997). Correspondingly, nucleus-hugging actin cables often occur in the vicinity of the SPB, e.g., in half of t = 4 hr nuclei (n = 34) (Figure 4Biii; Movie S26). This correspondence may explain the spatial bias of the "bouquet" (Discussion).

Figure 4. Actin Cables and Their Relationships to NE and Chromosome Movement

(A) Time series (Movie S24; strain YCT791) of the actin cable network (labeled with Abp140-GFP; left panel) and chromosomal mass (DAPI stained; middle panel). GFP (green) and DAPI (red) signals are merged and interesting features of the actin cable network, "black hole" (text) and DNA mass, are schematized with lines, red ellipse, and orange surface, respectively (right panel). Cables in contact with the chromosomal mass are outlined in green. Dotted line indicates the original position of the upper left side of the nuclei.

(B) Consecutive optical sections (0.2 μm × 600 ms) spanning an entire cell reveal the actin cable network in 3D. Schematic representations show the approximate localization of the NE (red dotted ellipse), as deduced by concomitant DAPI staining, and the actin network (gray lines). Cables in contact with the nucleus are outlined in colors and followed through successive sections. (i) Three-dimensional reconstruction of actin cables disposition along the nuclei; planes containing the bottom of the nucleus and of the cell are indicated by white arrowhead and dotted square, respectively. (ii) Schematic 3D reconstruction of a second nucleus. (iii) Position of a zygotene SPB labeled with SPC42-YFP (at 4 hr; NKY3999) relative to actin cables and corresponding schematic representation (Movie S26).

(C) Consecutive optical sections were extracted from live-cell 3D frame series at three different time points. NE and actin cables were colabeled with Nup49-GFP and Abp140-GFP, respectively (NKY3995), and their 3D organization (horizontally) was assessed as a function of time (vertically). Their relative disposition is outlined by white lines and schematized in red and green, respectively (green signal may eventually but unlikely be a thin NE protrusion). The dotted yellow line tracks the former position of the nucleus. The sections are close to the bottom of the cell, as schematized.

(D and E) Time series of the actin cable network (labeled with Abp140-GFP) and chromosomal mass (DAPI stained). (D) Top: merge images of GFP (green) and dapi (red) signals. The section framed by a white dotted box is magnified and schematized with actin in gray and DAPI-stained orphan in red. The dotted circles represent the position of the orphan in the former frame. (E) An actin fiduciary mark and an outward-directed chromosome are indicated by turquoise and yellow arrowheads, respectively. A pink arrowhead points at the localization of a secondary chromatin deformation. The bottom panel shows the chromatin outline (red circle) as well as the actin cable of interest (green line). The fiduciary mark is schematized as a green patch, the outward-directed chromosome as a yellow line, and the position of secondary chromatin movement as a pink asterisk. All cells were examined 5–6 hr after meiosis induction and all scale bars are 2 μm.

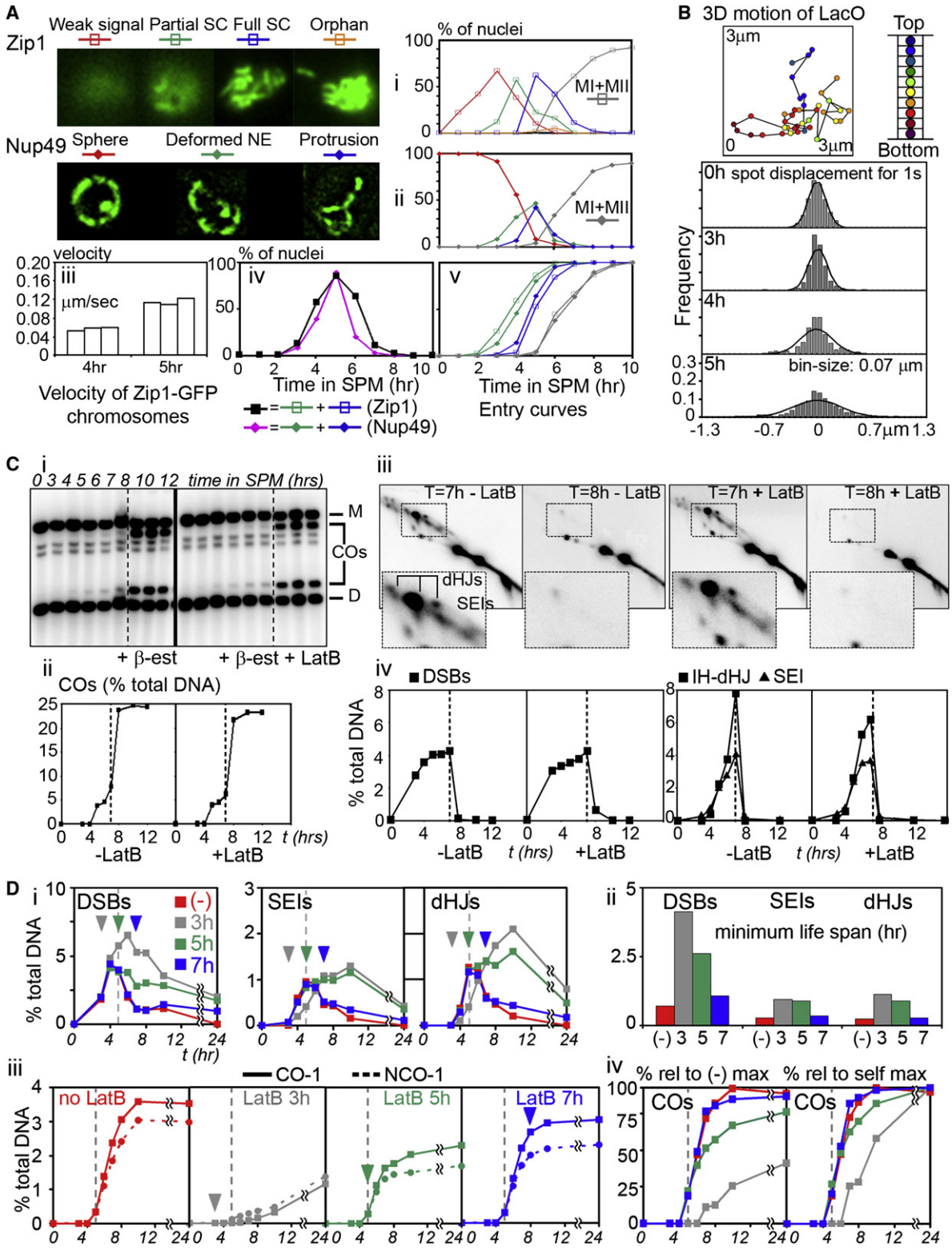

Figure 5. Timing, Quantification, and Potential Effects of Motion

(A) Categories of expanding SC (i) and NE deformations (ii), quantified over time during meiosis in cells expressing either Zip1-GFP or Nup49-GFP (NKY3834 and NKY3992, respectively; n = 100). Meiotic divisions (MI+MII) shown in gray. (iii) Mean velocities of random chromosomes (n = 30) tracked at 1 s intervals in three random nuclei during zygotene (4 hr) and pachytene (5 hr). (iv) Proportions of cells showing NE deformations (pink) and full or partial SC chromosomes (black)

Coordinately Dynamic Associations between Chromosomes and Actin Cables

Correlated Motion

Chromosome movements described above could be explained if, in each transition, a single telomere/NE complex associates with a nucleus-hugging actin cable; moves for a few seconds in conjunction with that cable; and then stops, without necessarily being released. Other chromosomes would move coordinately according to connectedness with this leader. Timelapse covisualization of Abp140-GFP and DAPI reveals sequences matching this description. In Figure 4E (Movie S27), a chromosome end is closely spatially associated with an actin cable (yellow triangle and corresponding yellow line below; t = 3 s). The end of this chromosome then moves, maintaining its association with the cable, for ~7 s (transition 1), pauses, remains in the vicinity of the cable for ~10 s, and then resumes its cable-associated movement for another ~7 s (transition 2). During this sequence, a second chromosome associates with the same cable and then moves in the same way (pink arrow and corresponding pink asterisk below). In all three transitions, ends move at ~0.2 μm/s. These images support the proposed model not only qualitatively but with respect to the frequency, velocity, and duration of movement. Such movies also confirm that telomere-led motion results in movement of other chromosomes. In Figure 4E, the overall chromatin pattern changes during the first period of telomere-led movement, does not change during the pause period, and then begins to change again thereafter, concomitant with later movements.

Covisualization movies also provide examples in which an orphan chromosome is associated with an actin cable through a period of dynamic changes, in correspondence to "dangling of orphans" (above). In Figure 4D, an isolated DAPI signal is associated with a "hook" in an actin cable and then remains associated as the hook changes shape and drifts (from right to left).

A Passive Attachment Mechanism

Covisualization movies also reveal that lead chromosome end appears to move via passive attachment to a cable that is, independently, being propelled through space. Movement of an actin cable within the nucleus is revealed by brightly staining "bulges" that remain fixed in position along the cable, thus providing "fiduciary marks" (Yang and Pon, 2002). In Figure 4E, in transition 1, the chromosome end can be seen to move in parallel with the indicated fiduciary mark (Figure 4E; yellow and turquoise triangles at top; yellow line and green bulge, bottom), implying that the end is remaining at a fixed position along the cable, while the cable itself is sliding along the surface of the NE and beyond, thereby mediating curvilinear, outward-directed movement of the associated chromosome end. Cable movement is thought to occur due to addition of subunits at various positions within the network. In further support of a passive attachment mechanism, typical rates of movement for leader chromosome ends correspond to the previously defined speed of actin cable extension (0.3–0.5 μm/s versus ~0.3 μm/s; Yang and Pon, 2002).

Chromosome and NE Movement Begin Coordinately at Zygotene

In yeast cultures undergoing synchronous meiosis, the zygotene and pachytene stages (nuclei with forming and formed SC; Introduction) occur sequentially, as seen, e.g., by analysis of Zip1-GFP patterns (Figure 5Ai). The timing with which cells enter and exit each stage is given by cumulative curve analysis (Hunter and Kleckner, 2001; Figure 5Av). Parallel analysis of Nup49-GFP dynamics reveals that NE deformations begin at zygotene and become more pronounced at pachytene, with long protrusions limited to the latter period (Figures 5Aii, 5Aiv, and 5Av). Chromosome movement exhibits the same progression. Motion was examined independently of the SC via a telomere-localized *lacO*-LacI-GFP array and via monitoring of Zip-GFP (Experimental Procedures). Step-size distributions of focus displacements reveal that mobility is unchanged from onset of meiosis (t = 0) through leptotene (t = 3 hr), increases significantly at zygotene (t = 4 hr), and is even more dramatic at pachytene (t = 5 hr) (Figures 5Aiii and 5B). Interestingly, even though onset of zygotene is tightly linked to a key step of meiotic recombination, motion initiates at approximately the usual time in mid-prophase even in the absence of recombination, as seen by analogous analysis in a *spo11Δ* mutant (data not shown). In WT meiosis, onset of motion may be part of the basic cellular program that becomes coupled to progression of recombinational progression by coordinating regulatory mechanisms.

LatB Disrupts Early Postinitiation Steps of Recombination

Programmed DNA recombination, a prominent feature of meiosis (Bishop and Zickler, 2004), initiates at early prophase (leptotene) via programmed double-strand breaks (DSBs). At late leptotene, some DSBs are designated to mature into crossover (CO) recombination products; the remainders are fated for maturation

(same timecourses as in i and ii, respectively). (v) Cumulative analysis showing when cells exhibiting NE deformations or onset of SC formation, detailed in (i) and (ii), have entered the corresponding stage.

(B) Top: 3D trajectory of a telomeric *lacO*/lacI-GFP spot (NKY3835). Bottom: step-size distribution histograms of the 2D displacement of projected *lacO*/lacI-GFP signal, tracked every second for 2 min in three random nuclei at 0, 3, 4, and 5 hr in sporulation medium (SPM). Predicted normal distributions are indicated.

(C) Meiotic recombination in *ndt80Δ*-arrested cells, released from arrest at t = 7 hr in the presence or absence of LatB (NKY3889). Recombination analyzed at *HIS4LEU2* as described (Hunter and Kleckner 2001; Experimental Procedures). (i) Parental homologs, "Dad" (D) and "Mom" (M), DSBs, and COs are distinguished on Southern blots via restriction site polymorphism. (ii and iv) DNA species as percent of total hybridizing signal with time after transfer to SPM. (iii) Representative 2D gels of SEIs and dHJs from the timecourses shown in (i).

(D) Effect of LatB on recombination progression (NKY3990). Arrowheads indicate the time of LatB addition to aliquots of a same premeiotic culture (color code corresponds to no addition [–], addition at t = 3, 5, and 7 hr). Dotted line at 5 hr helps graph to graph comparison. (i) Quantification of DSB, SEI, and dHJ species over time and (ii) corresponding life spans (i.e., time when 50% of the initiated recombination events have entered or exited the corresponding stage). (iii) CO and NCO formation as percent of total hybridizing signal in LatB timecourse experiments. (iv) Left panel: CO level relative to the maximum level observed in the control culture (–). Right panel: for each culture, relative CO levels when compared to the maximum level observed in the corresponding culture.

into noncrossovers (NCOs). CO designation also locally nucleates SC formation (onset of zygotene). For CO recombination, the two DSB ends interact sequentially with a partner DNA segment, giving single-end invasions (SEIs) during zygotene and then, during pachytene, double Holliday junctions (dHJs) that mature into products.

To ask whether chromosome motion might be important for recombination, we first used a system in which a transcription factor required for late stages of CO formation, Ndt80, is expressed from a hormone-inducible promoter (Benjamin et al., 2003). Recombination was assayed at the well-characterized *HIS4LEU2* hot spot (Hunter and Kleckner, 2001). Prior to Ndt80 expression, dHJs and some SEIs accumulate while COs are rare. When hormone is added, intermediates disappear, and COs appear, extremely rapidly (Figure 5C). If LatB is added concomitantly with hormone, chromosome movement stops immediately (data not shown) but completion of CO formation is absolutely unaffected (Figure 5C, compare +LatB with −LatB for all panels). Thus, motion is not required for these zygotene/pachytene events.

To probe for earlier effects, we added LatB to cells proceeding synchronously through meiosis at various times during the process (see Figure S3). Addition at t = 3 hr, when many DSBs have formed but no later species are present (Figure 5Di), confers delayed turnover of DSBs, SEIs, and dHJs, as shown by increases in the "life spans" of these species (Hunter and Kleckner, 2001; Figure 5Dii). Also, CO and NCO products form at reduced levels and with delayed timing (Figures 5Diii and 5Div). Thus, LatB *can* disrupt recombination if added early enough. Addition of LatB at t = 0 has a similar effect to addition at t = 3 hr (data not shown), suggesting that the early events of DNA replication and DSB formation are not LatB/motion sensitive (data not shown). Thus, the period of direct LatB sensitivity is mid-late leptotene through early pachytene, consistent with a role for zygotene/pachytene movement in recombination.

There appear to be three distinct effects of LatB on recombination. (1) Addition of LatB at t = 3 hr differentially affects CO formation versus NCO formation and severely reduces both types of products. This phenotype closely resembles that conferred by absence of Ndt80 (Figure 5C and K.P.K., unpublished data) and thus could reflect an indirect effect of LatB on transcription. (2) Addition of LatB at t = 5 hr coordinately affects both CO and NCO products, which are modestly reduced in level and modestly delayed in timing (Figures 5Diii and 5Div). This phenotype resembles that conferred by absence of Ndj1/Csm4 and thus reflects loss of motion per se (Discussion). (3) LatB affects pachytene steps when added at or before zygotene (t = 4 hr) but not when added directly to pachytene (*ndt80Δ*-arrested) cells. Thus, pachytene defects occur only as an indirect consequence of earlier problems.

DISCUSSION

The current study provides new information about the mechanics and movement of budding yeast meiotic chromosomes and points to a possible role for movement in resolution of topological irregularities among pairing chromosomes.

Meiotic Pachytene Chromosomes Are Semiflexible Objects

The current study provides an experimental assessment of the thermal persistence length of a meiotic pachytene chromosome. The obtained value of ~10 μm implies that these chromosomes are semiflexible objects. The stiffness represented by this value could be determined primarily by properties of the (structurally prominent) SC. However, a more intriguing possibility is that the primary determinant is the state of the chromatin. This possibility arises because bending of the SC requires compression of the chromatin along the inner surface of the bend and thus could be limited by the stiffness of that chromatin (Almagro et al., 2004; Marko and Siggia, 1997; Kleckner et al., 2004; below). Indeed, a ~10 μm persistence length is close to that predicted by a "bottle-brush" polymer model for meiotic pachytene chromosomes in which axis stiffness makes no contribution (Marko and Siggia, 1997; data not shown). The fact that Lp = ~10 μm is also interesting because it is similar to that of actin filaments (~17 μm; Ott et al., 1993), consistent with mechanical interplay between the chromosomes and nucleus-hugging actin cables.

How Do Pachytene Chromosomes Move?

Zygotene/pachytene chromosome motion requires both actin and telomere/NE association (references above; this work). We now find that motion involves cytoskeletal actin cables, rather than intranuclear actin as sometimes proposed. We find specifically that segments of the cytoskeletal actin network are intimately associated with the NE and that complexes involving both chromosome ends and their associated NE regions move along these nucleus-hugging cables, with concomitant deformation of the NE and nearby chromosomes (Figure 6A).

A "Piggy-Backing" Mechanism

We present evidence that motion occurs by passive association of telomere/NE complexes to these cables that are, irrespective of such association, moving dynamically through the cytoplasm. This "piggy-backing" mechanism is analogous to that proposed for movement of mitochondria through the cytoplasm in yeast (Fehrenbacher et al., 2004). Other mechanisms described for actin-mediated movement are: (1) cargo transport mediated by motor proteins and (2) direct actin polymerization on the object itself. A motor mechanism is unlikely here because it does not predict coordinate movement of chromosome ends with fiduciary marks. A directed polymerization model is unlikely as it would place the moving object at the ends of, rather than along, actin tracks.

An Integrated Mechanical System

When force is exerted on the NE component of the telomere/NE complex, that motion is constrained by linkages within the system. Those linkages ultimately undergo local mechanical disruption. (1) The lengths of the longest chromosomal protrusions match that of pachytene bivalents (1.1 ± 0.5 μm [n = 10] and 1.1 ± 0.35 μm [n = 30], respectively), suggesting that outward-directed movement is limited by anchoring of the distal end, e.g., to the NE. (2) Long NE protrusions, in contrast, are usually much longer (2.1 ± 0.7 μm, n = 34), suggesting that once chromosome extension is limited, the NE portion of the telomere complex often dissociates and continues to move outward. (3) Orphans separate from the main chromosome complement at

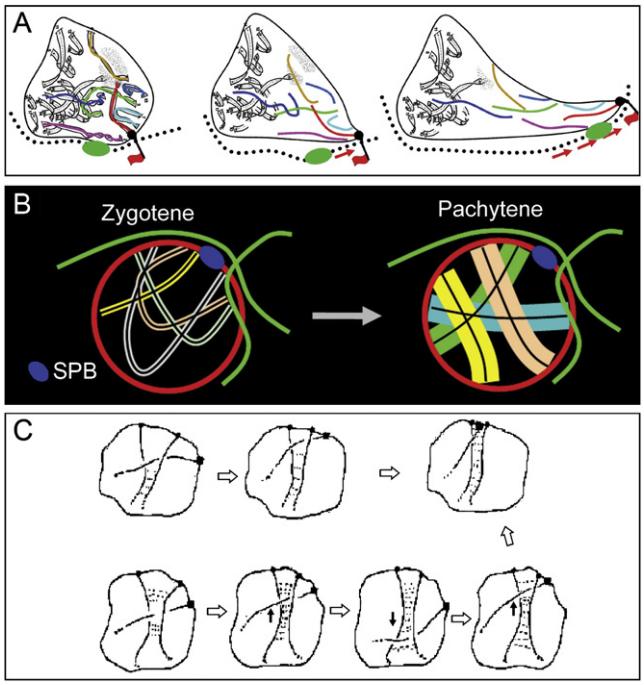

Figure 6. Zygotene/Pachytene Chromosome Dynamics

(A) "Piggy-back" model for pachytene movements. Background image is the serial reconstruction of SC fragment of *S. cerevisiae* from Byers and Goetsch (1975; Figure 2). Outline of NE was added on the cartoon, and a subset of bivalents was colorized to facilitate monitoring. A chromosome/NE complex (black ball) binds passively along a nucleus-hugging actin cable (red flag). The cable moves/slides, as indicated by movement of the fiduciary mark (green thickening), dragging the telomere/NE complex in parallel, and concomitantly causing a local deformation of the NE. Intermingled chromosomes move coordinately.

(B) Thinner zygotene chromosomes (left) are able to have multiple telomeres simultaneously associated with nucleus-hugging actin cables (thus can colocalize with one another in the vicinity of the SPB) whereas fat, stiff pachytene chromosomes (right) can attach only one at a time and, additionally, can not coaggregate.

(C) Interlocks could be resolved via movement of chromosome ends with accompanying adjustment of synapsis, in response and/or as a driving force (from Kleckner and Weiner, 1993; Copyright holder is Cold Spring Harbor Laboratory Press).

distances matching the maximum protrusion distance (2.3 ± 1.1 μm, n = 6 orphans), suggesting that orphans arise when a moving chromosome loses its distal constraints. (4) NE deformations arise as cones that often evolve into longer or shorter protrusions. This pattern implies initial resistance from the membrane and its substructure (matrix and/or chromatin) followed by dissociation from the substructure and elongation into a (chromosome-containing) membrane tube. (4) Coordinate movement of spatially associated chromosomes could involve direct interchromosomal linkages (e.g., as in mitotic chromosomes; reviewed in Poirier and Marko, 2003) and/or coassociation of ends to a common area of interconnected NE-embedded proteins, e.g., Mps3/Csm4, which exhibit patchy NE staining (Conrad et al., 2007, 2008; B. Weiner, personal communication).

Reconciling Zygotene and Pachytene

As a specific feature of the yeast zygotene stage, chromosome ends tend to colocalize near but not at the SPB (the bouquet configuration); at pachytene, ends are distributed relatively evenly throughout the nuclear periphery. Movements involved in this progression are presumably provided by actin-mediated telomere-led movement, which occurs specifically at these two stages. What, then, determines the spatial localization at zygotene and the abrogation of that localization at pachytene? The current work provides an important clue: nucleus-hugging actin cables tend to occur preferentially near, but not at, the SPB and near the edge of the cell, thus explaining how dynamic movements can have the zygotene spatial bias. Moreover, since pachytene chromosome movement involves tracks and preferred focal points, the same spatial bias likely occurs also at that stage but with single chromosome ends involved. Thus, the determinative difference between the two stages is the state of the chromosomes rather than the nature of motion.

We propose that the zygotene/pachytene progression is directly driven by changes in chromatin compaction. In many organisms, including yeast, chromatin is more compact at zygotene and more expanded at pachytene (Kleckner et al., 2004). More compact chromatin will make chromosomes not only more compact but also floppier (above), thus permitting closer juxtaposition of multiple chromosome ends into the bouquet (Figure 6B, left panel). Expansion of chromatin at early pachytene will then produce fatter, stiffer chromosomes that can only behave independently, like sausages contained within a small sphere (Figure 6B, right panel; see also Figures 3B and 4E; Note S2 and Figure S4).

Role(s) of Actin-Mediated Mid-Prophase Motion

The bouquet phenomenon has long been discussed in relation to the overall dynamics of homolog pairing and juxtaposition. Classically the bouquet was thought to promote initial homolog contacts by reducing the dimensionality of homology searching. Similarly, dynamic chromosome movements might provide "stirring forces" needed to bring corresponding regions into spatial proximity.

An alternative possibility is that chromosome movement, over short and long time scales, is required to help prevent topological entanglements during the latter stages of homolog juxtaposition and to eliminate such entanglements if they remain into the pachytene stage (for previous discussions see Rasmussen, 1986; Scherthan et al., 1994). We favor this view. We propose specifically that movement permits an entrapped chromosome to be released by sliding out to the end(s) of the entrapping chromosomes (Figure 6C). In support of this idea: (1) The dynamic movements in the three published examples are all of a "back-and-forth" character, "rotationally" in rat (Parvinen and Soderstrom, 1976), along the length of the nucleus in *S. pombe* (Chikashige et al., 2007), and along actin cables in *S. cerevisiae* (above). These are not the effects required for "stirring" but are exactly what is needed for resolution of entanglements or other types of nonspecific connections. (2) Primary homolog recognition has already occurred before movement begins (Zickler, 2006; Hunter and Kleckner, 2001).

Correspondingly, stirring forces needed for juxtaposition can be provided by basal movement known to occur even in mitotic G1 cells (Introduction). (3) This model can explain how abrogation of motion might affect recombination during early post-DSB stages (above). An irregular topological relationship will preclude the occasional DSB from finding or then mediating close juxtaposition of chromosome axes. Such a defect should be sensed by the cell, not as "damage," but as "not ready to progress," resulting in a global temporal delay without (necessarily) any major defect in product formation. The milder effect of LatB on recombination is of this nature, as is that conferred by *ndj1* or *csm4* mutation(s) (Conrad et al., 2008; K.P.K., unpublished data; A Shinohara, personal communication). Long-term persistence of incomplete interactions might then confer regulatory delays at later stages, thus explaining the indirect effects of LatB on pachytene events. (4) A maize mutant defective in bouquet colocalization of NE-associated telomeres (perhaps analogously to *csm4Δ* above) shows an increase in pachytene interlocks (Golubovskaya et al., 2002).

An additional, not mutually exclusive, role for motion might be to eliminate nonspecific connections between unrelated chromosomes, e.g., involving their peripheral chromatin. Spindle-associated movements might play analogous roles during prometaphase/metaphase of mitosis and the meiotic divisions. Moreover, since residual motion is still manifested for non-telomere-associated (*ndj1Δ*) chromosomes, movement mediated by NE-associated cytoskeletal actin cables (passively or via motors) could promote chromosome movement even in the absence of specific telomere/NE complexes. And such motions, by loosening connections between/within chromosomes, might promote the types of dynamic motions involved in basic cellular processes (Introduction).

Summary

Taken together the above findings permit a coherent model in which, concomitant with the latter stages of homolog juxtaposition, telomere-led movement in combination with compaction and expansion of chromatin produces an overall dynamic whose primary role is regularization of topological relationships among pairing chromosomes.

EXPERIMENTAL PROCEDURES

Strains and Meiotic Timecourses

Yeast strains are isogenic *MATa/MATα* derivatives of wild-type SK1 (Table S1). Details on strains constructions are available in the Supplemental Data (Note S3). Pregrowth and synchronous meiosis are as described, with all media equilibrated to 30°C prior to use, and synchrony of DNA replication and divisions monitored (Hunter and Kleckner, 2001).

Analysis of Isolated Pachytene Chromosomes In Vitro

Yeast cells of pachytene stage were spheroplasted (Keeney et al., 1997) and resuspended in spheroplast buffer (0.4 M sorbitol, 0.4 M KCl, 40 mM dipotassium phosphate, 0.5 mM $MgCl_2$, Sigma Protease inhibitor cocktail P8215 1:300). One microliter was loaded on the glass slide (plain, nontreated) at room temperature, gently mixed with 6 μl of distilled water, and covered with a coverslip and incubated at room temperature for ~20 min.

Chemical Treatments of Pachytene Cells

All chemicals are from Sigma and were dissolved in dimethyl-sulfoxide (DMSO). Cell aliquots of interest were incubated in 30 μM Latrunculin A or B 3 or 15 min prior to timelapse, 40 μM CCCP (20 min at 30°C to deplete pre-existing ATP), 15 μg/ml nocodazole (20 min at 30°C), and BDM 200 μm to 100 mM (15 min at 30°C) (Heun et al., 2001). Control aliquots treated with DMSO (up to 1% final concentration) always exhibit motions similar to nontreated cells.

NDT80 Arrest and Release

A single culture of NKY3889 was synchronized and fractionated into two identical sporulation cultures in 1% potassium acetate and 0.02% raffinose. At t = 7 hr, 1 μm β-estradiol (Sigma) was added to both cultures to release mid-prophase arrest. In one culture, fresh 15 μM LatB (Sigma) was concomitantly added. DNA events were analyzed as in Hunter and Kleckner (2001; Probe "A").

In Vivo DAPI Staining of Chromosomes

DAPI (Sigma) was directly added to cell samples to a final concentration of 10–20 μg/ml. After incubation overnight on ice, ~10% of cells present faintly stained chromosomes, all still showing dynamic movements. Analysis of Zip1-GFP chromosomes confirms that DAPI treatment does not affect chromosome motion.

Live-Cell Imaging

Cell samples were vortexed at full speed for 10 s and ~3 μl quickly spread onto a glass slide (plain, nontreated). A 22 × 22 mm coverslip was added in such a way that several air bubbles remain trapped, with cells located in their vicinity (up to ~30 μm) exhibiting motion for a few minutes. This oxygenation is crucial: motion quickly stops if the air bubble drifts away from an observed cell. Cells are observed at room temperature using an epifluorescence microscope (Zeiss) equipped with GFP, DAPI, and TexRed filters, a Cascade 512b CCD camera (Roper Scientific), and a PIFOC piezo device (Physik Instrumente) to drive a 100× oil immersion objective (NA 1.45) for acquiring Z stacks. Images were acquired using Metamorph software. Two color movies were made from sequential acquisition of frames alternating with switch of filters, generating a ~300 ms discrepancy between two superimposed frames.

Image Analysis

Deconvolution of 2D and 3D acquisitions was performed using AutoDeblur. For bending and step-size studies, outlines of Zip1-GFP chromosomes were drawn by thresholding and centroids automatically determined by the Integrated Morphometry Analysis function of Metamorph. For tracking of LacO-telomeres, Z stacks time series were recorded every 3 s during 3 min, planes separated by 0.20 μm (21 total). For each plane, X and Y coordinates of the LacI-GFP spot centroid were calculated by SpotTracker2D ImageJ Plug-in (Sage et al., 2005). The Z coordinate of the spot was approximated as coordinate of the plane containing the brightest centroid. Velocities were calculated from relative positions of spots in successive Z series (three independent nuclei per time point).

SUPPLEMENTAL DATA

Supplemental Data include three supplemental notes, four figures, one table, and twenty-seven movies and can be found with this article online at http://www.cell.com/cgi/content/full/133/7/1188/DC1/.

ACKNOWLEDGMENTS

We thank A. Shinohara, E. Alani, J. Wanat, and M. Dresser for unpublished data; A. Amon, J. Fung, E. White, S. Gasser, I. Nachman, K. Thorn, A. Murray, K. Nasmyth, and D. Knop for plasmids/strains; and B. Byers, R. Padmore, and D. Zickler for reproduction of images in Figures 6 and S4. Support for M.P. was provided by Harvard University. R.K., S.K., K.P.K., and this research were supported by grants to N.K. (NIH RO1 GM-044794 and/or NIH RO1 GM-025326).

Received: October 17, 2007
Revised: February 8, 2008
Accepted: April 22, 2008
Published: June 26, 2008

REFERENCES

Agarwal, S., and Roeder, G.S. (2000). Zip3 provides a link between recombination enzymes and synaptonemal complex proteins. Cell *102*, 245–255.

Almagro, S., Riveline, D., Hirano, T., Houchmandzadeh, B., and Dimitrov, S. (2004). The mitotic chromosome is an assembly of rigid elastic axes organized by structural maintenance of chromosomes (SMC) proteins and surrounded by a soft chromatin envelope. J. Biol. Chem. *279*, 5118–5126.

Bass, H.W. (2003). Telomere dynamics unique to meiotic prophase: formation and significance of the bouquet. Cell. Mol. Life Sci. *60*, 2319–2324.

Belgareh, N., and Doye, V. (1997). Dynamics of nuclear pore distribution in nucleoporin mutant yeast cells. J. Cell Biol. *136*, 747–759.

Benjamin, K.R., Zhang, C., Shokat, K.M., and Herskowitz, I. (2003). Control of landmark events in meiosis by the CDK Cdc28 and the meiosis-specific kinase Ime2. Genes Dev. *17*, 1524–1539.

Bishop, D.K., and Zickler, D. (2004). Early decision; meiotic crossover interference prior to stable strand exchange and synapsis. Cell *117*, 9–15.

Byers, B., and Goetsch, L. (1975). Electron microscopic observations on the meiotic karyotype of diploid and tetraploid Saccharomyces cerevisiae. Proc. Natl. Acad. Sci. USA *72*, 5056–5060.

Chikashige, Y., Haraguchi, T., and Hiraoka, Y. (2007). Another way to move chromosomes. Chromosoma *116*, 497–505.

Conrad, M.N., Dominguez, A.M., and Dresser, M.E. (1997). Ndj1p, a meiotic telomere protein required for normal chromosome synapsis and segregation in yeast. Science *276*, 1252–1255.

Conrad, M.N., Lee, C.Y., Wilkerson, J.L., and Dresser, M.E. (2007). MPS3 mediates meiotic bouquet formation in *Saccharomyces cerevisiae*. Proc. Natl. Acad. Sci. USA *104*, 8863–8868.

Conrad, M.N., Lee, C.-Y., Chao, G., Shinohara, M., Kosaka, H., Shinohara, A., Conchello, J.-A., and Dresser, M.E. (2008). Rapid telomere movement in meiotic prophase is promoted by *NDJ1*, *MPS3*, and *CSM4* and is modulated by recombination. Cell *133*, this issue, 1175–1187.

Doi, M., and Edwards, S.F. (1986). The Theory of Polymer Dynamics (Oxford, UK: The Clarendon Press).

Fehrenbacher, K.L., Yang, H.C., Gay, A.C., Huckaba, T.M., and Pon, L.A. (2004). Live cell imaging of mitochondrial movement along actin cables in budding yeast. Curr. Biol. *14*, 1996–2004.

Golubovskaya, I.N., Harper, L.C., Pawlowski, W.P., Schichnes, D., and Cande, W.Z. (2002). The pam1 gene is required for meiotic bouquet formation and efficient homologous synapsis in maize (Zea mays L.). Genetics *162*, 1979–1993.

Harper, L., Golubovskaya, I., and Cande, W.Z. (2004). A bouquet of chromosomes. J. Cell Sci. *117*, 4025–4032.

Heun, P., Laroche, T., Raghuraman, M.K., and Gasser, S.M. (2001). The positioning and dynamics of origins of replication in the budding yeast nucleus. J. Cell Biol. *152*, 385–400.

Hunter, N., and Kleckner, N. (2001). The single-end invasion: an asymmetric intermediate at the double-strand break to double-holliday junction transition of meiotic recombination. Cell *106*, 59–70.

Keeney, S., Giroux, C.N., and Kleckner, N. (1997). Meiosis-specific DNA double-strand breaks are catalyzed by Spo11, a member of a widely conserved protein family. Cell *88*, 375–384.

Kleckner, N., and Weiner, B.M. (1993). Potential advantages of unstable interactions for pairing of chromosomes in meiotic, somatic, and premeiotic cells. Cold Spring Harb. Symp. Quant. Biol. *58*, 553–565.

Kleckner, N., Zickler, D., Jones, G.H., Dekker, J., Padmore, R., Henle, J., and Hutchinson, J. (2004). A mechanical basis for chromosome function. Proc. Natl. Acad. Sci. USA *101*, 12592–12597.

Klein, F., Laroche, T., Cardenas, M.E., Hofmann, J.F., Schweizer, D., and Gasser, S.M. (1992). Localization of RAP1 and topoisomerase II in nuclei and meiotic chromosomes of yeast. J. Cell Biol. *117*, 935–948.

Kumaran, R.I., Thakar, R., and Spector, D.L. (2008). Chromatin dynamics and gene positioning. Cell *132*, 929–934.

Marko, J.F., and Siggia, E.D. (1997). Polymer models of meiotic and mitotic chromosomes. Mol. Biol. Cell *8*, 221722–221731.

Ott, A., Magnasco, M., Simon, A., and Libchaber, A. (1993). Measurement of the persistence length of polymerized actin using fluorescence microscopy. Phys. Rev. E Stat. Phys. Plasmas Fluids Relat. Interdiscip. Topics *48*, R1642–R1645.

Parvinen, M., and Soderstrom, K.O. (1976). Chromosome rotation and formation of synapsis. Nature *260*, 534–535.

Poirier, M.G., and Marko, J.F. (2003). Micromechanical studies of mitotic chromosomes. Curr. Top. Dev. Biol. *55*, 75–141.

Rasmussen, S.W. (1986). Initiation of synapsis and interlocking of chromosomes during zygotene in *Bombyx* spermatocytes. Carlsberg Res. Commun. *51*, 401–432.

Sage, D., Neumann, F.R., Hediger, F., Gasser, S.M., and Unser, M. (2005). Automatic tracking of individual fluorescence particles: application to the study of chromosome dynamics. IEEE Trans. Image Process. *14*, 1372–1383.

Scherthan, H. (2007). Telomere attachment and clustering during meiosis. Cell. Mol. Life Sci. *64*, 117–124.

Scherthan, H., Bähler, J., and Kohli, J. (1994). Dynamics of chromosome organization and pairing during meiotic prophase in fission yeast. J. Cell Biol. *127*, 273–285.

Scherthan, H., Wang, H., Adelfalk, C., White, E.J., Cowan, C., Cande, W.Z., and Kaback, D.B. (2007). Chromosome mobility during meiotic prophase in Saccharomyces cerevisiae. Proc. Natl. Acad. Sci. USA *104*, 16934–16939.

Shaw, S.L., Yeh, E., Maddox, P., Salmon, E.D., and Bloom, K. (1997). Astral microtubule dynamics in yeast: a microtubule-based searching mechanism for spindle orientation and nuclear migration into the bud. J. Cell Biol. *139*, 985–994.

Taxis, C., Maeder, C., Reber, S., Rathfelder, N., Miura, K., Greger, K., Stelzer, E.H., and Knop, M. (2006). Dynamic organization of the actin cytoskeleton during meiosis and spore formation in budding yeast. Traffic *7*, 1628–1642.

Trelles-Sticken, E., Dresser, M.E., and Scherthan, H. (2000). Meiotic telomere protein Ndj1p is required for meiosis-specific telomere distribution, bouquet formation and efficient homologue pairing. J. Cell Biol. *151*, 95–106.

Trelles-Sticken, E., Adelfalk, C., Loidl, J., and Scherthan, H. (2005). Meiotic telomere clustering requires actin for its formation and cohesin for its resolution. J. Cell Biol. *170*, 213–223.

Yamamoto, A., West, R.R., McIntosh, J.R., and Hiraoka, Y. (1999). A cytoplasmic dynein heavy chain is required for oscillatory nuclear movement of meiotic prophase and efficient meiotic recombination in fission yeast. J. Cell Biol. *145*, 1233–1249.

Yang, H.C., and Pon, L.A. (2002). Actin cable dynamics in budding yeast. Proc. Natl. Acad. Sci. USA *99*, 751–756.

Zickler, D. (2006). From early homologue recognition to synaptonemal complex formation. Chromosoma *115*, 158–174.

Zickler, D., and Kleckner, N. (1998). The leptotene-zygotene transition of meiosis. Annu. Rev. Genet. *32*, 619–697.